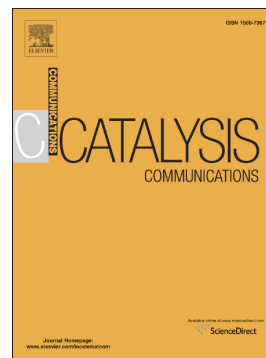


## Accepted Manuscript

Effect of Mo loading on 2-naphthaldehyde formation from vapor phase oxidation of 2-methylnaphthalene with V<sub>2</sub>O<sub>5</sub>/TiO<sub>2</sub> catalysts

Xiaoqiang Gao, Fang Zhang, Yi Yu, Yonghui Dou, Li Xu, Guoji Liu



PII: S1566-7367(18)30592-2

DOI: <https://doi.org/10.1016/j.catcom.2018.12.019>

Reference: CATCOM 5582

To appear in: *Catalysis Communications*

Received date: 7 October 2018

Revised date: 16 December 2018

Accepted date: 28 December 2018

Please cite this article as: Xiaoqiang Gao, Fang Zhang, Yi Yu, Yonghui Dou, Li Xu, Guoji Liu, Effect of Mo loading on 2-naphthaldehyde formation from vapor phase oxidation of 2-methylnaphthalene with V<sub>2</sub>O<sub>5</sub>/TiO<sub>2</sub> catalysts. *Catcom* (2018), <https://doi.org/10.1016/j.catcom.2018.12.019>

This is a PDF file of an unedited manuscript that has been accepted for publication. As a service to our customers we are providing this early version of the manuscript. The manuscript will undergo copyediting, typesetting, and review of the resulting proof before it is published in its final form. Please note that during the production process errors may be discovered which could affect the content, and all legal disclaimers that apply to the journal pertain.

**Effect of Mo loading on 2-naphthaldehyde formation from vapor phase oxidation  
of 2-methylnaphthalene with V<sub>2</sub>O<sub>5</sub> /TiO<sub>2</sub> catalysts**

Xiaoqiang Gao<sup>1</sup>, Fang Zhang<sup>2</sup>, Yi Yu<sup>1</sup>, Yonghui Dou<sup>1</sup>, Li Xu<sup>1\*</sup>, Guoji Liu<sup>1\*</sup>

<sup>1</sup> *School of Chemical Engineering and Energy, Zhengzhou University, No.100 Science Avenue, Zhengzhou 450001, China*

<sup>2</sup> *School of Environmental and Municipal Engineering, North China University of Water Resources and Electric Power, No.36 Beihuan Road, Zhengzhou 450045, China*

Corresponding author: Li Xu, xuli@zzu.edu.cn; Guoji Liu, guojiliu@zzu.edu.cn

**Abstract**

Mo-modified  $V_2O_5/TiO_2$  catalysts were prepared by wetness impregnation method and investigated for the selective oxidation of 2-methylnaphthalene to 2-naphthaldehyde. The catalysts were characterized by XRD, BET, XPS, and Raman to investigate the promotional effect of Mo on catalyst structure, surface property, and catalytic performance. The introduction of molybdenum decreases the amount of  $KVO_3$  phase and enhances the dispersion of the vanadium phase. XPS and Raman results indicate that Mo prevents Sn and K to interact with V species and bonds with Ti or V through bridge oxygen. V1Mo1 sample demonstrates a remarkable improvement in conversion and selectivity compared with others.

**Keywords:**  $V_2O_5/TiO_2$ ; Mo; 2-methylnaphthalene; 2-naphthaldehyde; vapor phase oxidation

## 1. Introduction

Supported vanadium oxide has been widely used as catalysts for methyl aromatics oxidation over the past few decades, such as oxidation of toluene, o-xylene, and 2-methylnaphthalene [1-4]. The transformation of 2-methylnaphthalene to 2-methyl-1,4-naphthoquinone and 2-naphthaldehyde under oxygen atmosphere has been developed over silica [4], alumina [5], or titania [6] supported vanadium oxide catalysts. Both of them are valuable chemicals and widely used in the field of plant regulators, antitumor drugs, vitamins of the K group and so on [7-9]. The synthesis of 2-methyl-1,4-naphthoquinone on  $V_2O_5$ - $K_2SO_4$ - $SiO_2$  catalyst with air as oxidant under high temperature has achieved a pretty good yield [4]. However, there still requires much effort to be done for catalytic synthesis of 2-naphthaldehyde. Otherwise, in the traditional manufacture of 2-naphthaldehyde, chlorine-containing wastewater produced costs a large amount of treatment fee. Therefore, it is urgent to develop a new clean production process and novel catalysts to solve this problem.

Recently, we have found that  $V_2O_5/TiO_2$  catalyst has good selectivity for 2-naphthaldehyde. However, conversion of 2-methylnaphthalene was about 45% for  $V_2O_5/TiO_2$  catalyst. According to Martin [10,11], the oxidation of methyl aromatics to their aldehydes strongly depends on the nature, strength, and concentration of acidic and basic surface sites of the catalysts and the acid-base properties of the reaction mixture. Early studies [12-14] indicates that addition of  $SO_4^{2-}$  and alkali cations ( $Li^+$ ,  $Na^+$ ,  $K^+$ ,  $Rb^+$ , and  $Cs^+$ ) increases the acidity and basicity of vanadia-titania catalysts, respectively. The amounts of  $K_2SO_4$  have an important effect on transformation of 2-methylnaphthalene to 2-naphthaldehyde for vanadia-titania catalysts.

$MoO_3$  is also an important catalytic agent for oxidation of hydrocarbons. Bertinchamps et al. [15] demonstrated that the incorporation of  $MoO_x$  into  $V_2O_5/TiO_2$  catalyst enhances the activity for the oxidation of benzene, and  $MoO_x$  phases induce a synergetic effect with  $VO_x$ . The simultaneous impregnation of Mo and V brings beneficial effect than two-step impregnation. However, Matralis et al. [16] reported that the addition of molybdenum decreases the activity and selectivity of  $V_2O_5/TiO_2$  catalyst for the oxidation of toluene, and inhibits the interaction between vanadium and anatase  $TiO_2$ . So in the present investigation, for understanding the promotional effect on the activity of the catalyst, different amount of Mo was introduced into  $V_2O_5/TiO_2$  catalyst using ammonium heptamolybdate by impregnation. The promotional effect of Mo is examined by different characterization techniques including X-ray diffraction (XRD), Raman spectrum, BET (Brunauer–Emmett–Teller) surface area, and X-ray photoelectron spectroscopy (XPS) and activities of the

catalysts are tested by choosing oxidation of 2-methylnaphthalene as a model reaction.

## 2. Experimental

### 2.1 Catalyst preparation

Molybdenum and vanadium were deposited on the TiO<sub>2</sub> support using the wet impregnation method. In a typical procedure, a certain amount of H<sub>2</sub>C<sub>2</sub>O<sub>4</sub> (Kermel, China, AR) was dissolved in 10 mL deionized water, then NH<sub>4</sub>VO<sub>3</sub> (Aladdin, China, AR) and (NH<sub>4</sub>)<sub>6</sub>Mo<sub>7</sub>O<sub>24</sub>·4H<sub>2</sub>O (Sinopharm, China, AR) were added simultaneously to react for a while till no bubbles came out, and the required amount of K<sub>2</sub>SO<sub>4</sub>, K<sub>2</sub>S<sub>2</sub>O<sub>7</sub>, SnSO<sub>4</sub>, KH<sub>2</sub>PO<sub>4</sub>, and Na<sub>2</sub>B<sub>4</sub>O<sub>7</sub>·10H<sub>2</sub>O were added in sequence subsequently. Finally, 9.5 g TiO<sub>2</sub> support powder (Aladdin, China, AR) was introduced into the solution and stirred for half an hour. Excess water was rotary evaporated on the water bath. The obtained sample was oven dried at 110 °C for 10 h and calcined at 450 °C in air for 2 h. A series of Mo-V<sub>2</sub>O<sub>5</sub>/TiO<sub>2</sub> catalysts was prepared by tuning V/Mo molar ratio. The catalysts was denoted as V<sub>2</sub>O<sub>5</sub>/TiO<sub>2</sub> (without molybdenum) and V<sub>x</sub>Mo<sub>y</sub> (where x:y = 6:1, 3:1, 1:1, 2:3, 1:2). The vanadium loading and K/V molar ratio were fixed at 5.77% (wt) and 1.97 for each sample. The detail amounts of compounds were presented in ESI.

### 2.2. Catalyst characterization

Powder X-ray diffraction (XRD) patterns were determined on a Bruker AXS D8 Advance diffractometer with Cu-K $\alpha$  radiation ( $\lambda$ = 0.15406 nm). The BET surface area

and pore size were measured with a Quantachrome Autosorb-iQ-2 instrument by nitrogen adsorption-desorption at  $-196\text{ }^{\circ}\text{C}$ . The samples were degassed in vacuum at  $300\text{ }^{\circ}\text{C}$  for 4 h before  $\text{N}_2$  physisorption. Raman spectra were measured by JY Horiba LabRam HR800 Raman spectrometer under ambient conditions using 532 nm laser excitation. The spectra were recorded with a resolution of  $2.5\text{ cm}^{-1}$ , a collection time of 100 s and an accumulation of 1 scans. The X-ray photoelectron spectroscopy was measured with AXIS Supra (XPS) surface analysis instrument (Kratos Analytical Ltd, monochromated Al  $\text{K}\alpha$  radiation). The binding energies were calibrated by using the C1s peak at 284.8 eV. The obtained spectra were fitted by Gaussian-Lorentzian functional shape (80:20) and Shirley-type background subtraction. X-ray fluorescence (XRF) and temperature programmed desorption ( $\text{NH}_3$ -TPD) experiments were carried out and the details were shown in the ESI material.

### 2.3. Catalytic activity measurement

The catalytic gas-phase oxidation reactions were performed in a fixed-bed stainless steel reactor under atmospheric pressure. The scheme of the experimental set up was shown graphically in ESI. About 0.50 g catalyst (65-80 mesh, pressed and sieved) diluted with 2.50 g same particle size quartz was filled into the tube reactor (10 mm i.d.) between two quartz wool plugs. Then the reactant gas mixture (2-MN/ $\text{O}_2$  molar ratio=1:160) obtained by passing air through a heated flask with 2-methylnaphthalene was fed into the reactor using mass flow controllers. The effluent stream was absorbed by 1,4-dioxane solvent in a cold trap and analyzed offline by gas chromatography (GC7890B, Agilent) equipped with flame-ionization

detector every two hours. All the lines connecting the reactor were heated to 140 °C to prevent condensation of the products. Prior to the measurements, the catalysts were activated at 450 °C with an air flow (100 ml/min) for 2 h. The temperature was decreased to 340 °C and the flow was then switched to the reaction mixture. The activity test duration was about 120 h for all the catalysts. The feed flow and gas hourly space velocity (GHSV) was 0.05 g/h and 10000 h<sup>-1</sup>, respectively. 2-Methylnaphthalene conversion (X/mol-%) and 2-naphthaldehyde yield (Y/mol-%) were determined after the catalyst has achieved steady-state and given as an average of four runs. The carbon balance was maintained at (100 ± 10) %. Blank tests showed that the reactor walls were inert in terms of 2-methylnaphthalene oxidation over the temperature range studied.

### **3. Results and discussion**

#### **3.1. Structure and surface study of catalysts**

##### *3.1.1. XRD*

The XRD patterns of the catalysts were shown in Fig. 1. The diffraction peaks representing anatase TiO<sub>2</sub> (JCPDS, 21-1272) and very weak rutile TiO<sub>2</sub> (JCPDS, 21-1276) existed in all the samples, but there were no diffraction peaks related to MoO<sub>3</sub> or V<sub>2</sub>O<sub>5</sub> species. This indicates that Mo and V species were well dispersed or presented in amorphous phase. Notably, the peaks related to KVO<sub>3</sub> species in the V<sub>x</sub>Mo<sub>y</sub> catalyst samples decreases or disappears with increasing Mo content, suggesting Mo introduction affects the interaction between K and V.

### 3.1.2. BET surface area and pore size

Table 1 lists the textural parameters of each catalyst sample. From Table 1, the introduction of Mo species into  $V_2O_5/TiO_2$  catalyst increases the specific surface area first, then decreases it seriously. The average pore size and pore volume of  $V_xMo_y$  samples decrease with the increasing amount of Mo, which could be caused by gradually entering of molybdenum ion into the pore of  $TiO_2$  support.  $V_xMo_y$  catalysts possess smaller pore size than  $V_2O_5/TiO_2$  catalyst, which could be beneficial for desorption and diffusion of products in the catalytic gas-phase oxidation reaction.

Compared to the fresh catalyst, the used one's pore size and pore volume declined seriously, which was probably due to coke deposits produced during the catalytic reaction. After a long time running, coke deposits could be accumulated on the surface or interior of the catalyst. It could hinder the reaction process, causing the decrease in conversion and selectivity.

### 3.1.3. Raman

The Raman spectra of the  $V_2O_5/TiO_2$  sample and of the  $V1Mo1$  catalyst are shown in Fig. S1 (ESI). Both of them shows five bands at 139, 193, 392, 510, and 634  $cm^{-1}$ , due to the anatase  $TiO_2$  [17,18]. The band at 475 and 632  $cm^{-1}$  can be assigned to the  $SnO_2$  species [19] and the latter one is covered by the strong peaks at 634  $cm^{-1}$  belonging to  $TiO_2$ . No bulk  $MoO_3$  and  $V_2O_5$  bands in the Raman spectra are observed [20], consistent with the result of XRD. Additional weak scattering is observed in the spectral region 1100-800  $cm^{-1}$ , due to molybdenum oxide or vanadium oxide species.

The band at 872 and 932-942  $\text{cm}^{-1}$  can be assigned to the amorphous  $\text{KVO}_3$  [21]. The bands at 957  $\text{cm}^{-1}$  are due to the symmetric stretch of the  $\text{V}=\text{O}$  groups in the polymeric vanadium oxide [22]. The band at 983 and 1000-1016  $\text{cm}^{-1}$  can be assigned to K-doped species ( $\text{K}-\text{O}-\text{V}=\text{O}$  sites) and K-perturbed species ( $\text{K}\dots\text{O}=\text{V}$  sites) [21,23]. After doping molybdenum, the intensity of the band at 139  $\text{cm}^{-1}$  increases, indicating that molybdenum introduction affects the surface of the  $\text{TiO}_2$  support and the interaction of  $\text{TiO}_2$  with  $\text{V}_2\text{O}_5$ . There may exist interaction between Mo and  $\text{SnO}_2$  causing the decrease of peak intensity at 475  $\text{cm}^{-1}$ . The intensities of  $\text{KVO}_3$  and  $\text{K}-\text{O}-\text{V}=\text{O}$  sites decrease due to the interaction of Mo with  $\text{V}_2\text{O}_5$ , probably by substituting K to form new bridge bonds with V.

#### 3.1.4. XPS

The  $\text{V}_2\text{O}_5/\text{TiO}_2$  and V1Mo1 catalysts, before and after catalytic tests, were characterized by XPS spectroscopy to elucidate the influence of Mo on  $\text{V}_2\text{O}_5/\text{TiO}_2$  catalyst. The binding energies of V 2p<sub>3/2</sub>, Ti 2p<sub>3/2</sub>, O 1s, Sn 3d<sub>5/2</sub>, and Mo 3d<sub>5/2</sub> of all samples were listed in Table 2.

Figure S2 (ESI) shows the spectra of Ti 2p. The peak at ca. 458.7-459.0 eV of all the samples was ascribed to Ti 2p<sub>3/2</sub> for  $\text{Ti}^{4+}$  [17], without  $\text{Ti}^{3+}$  species existing on the surface. Notably, the peak for 2p<sub>3/2</sub> of  $\text{Ti}^{4+}$  shifted to higher values with about  $\Delta E = 0.3$  eV after Mo introduction. This indicated the electron transfer between Mo and  $\text{TiO}_2$ , namely interaction between Mo and  $\text{TiO}_2$  for V1Mo1catalyst.

The Mo 3d spectra in Fig. S3 (ESI) shows the two peaks at 233.0 (232.7) and 236.1 (235.8) eV, corresponding to 3d<sub>5/2</sub> and 3d<sub>3/2</sub> of  $\text{Mo}^{6+}$  [24]. After catalytic tests,

the peak moved to lower values with about  $\Delta E = 0.3$  eV, implying Mo participated in the catalytic reaction. As for Sn  $3d_{5/2}$  shown in Fig. S4 (ESI), the peaks at 487.4 and 486.3 eV corresponded to  $\text{Sn}^{4+}$  and  $\text{Sn}^{2+}$ , respectively [25]. After addition of Mo, there was only one peak at 486.8 eV for Sn  $3d_{5/2}$ , indicating that Mo inhibited the transformation of  $\text{Sn}^{2+}$  to  $\text{Sn}^{4+}$ .

The V  $2p_{3/2}$  spectra in Fig. S5 (ESI) were fitted with two peaks at 517.7 and 516.6 eV, which were the typical binding energy of  $\text{V}^{5+}$  and  $\text{V}^{4+}$  [18]. After the introduction of Mo, Ammonium heptamolybdate consumed part of oxalic acid, reducing the amount used to reduce  $\text{V}^{5+}$ , and decreased the ratio of  $\text{V}^{4+}/\text{V}^{5+}$ . Besides, the introduction of Mo inhibited the conversion of  $\text{V}^{5+}$  to  $\text{V}^{4+}$  via Sn ( $2\text{V}^{5+} + \text{Sn}^{2+} \rightarrow 2\text{V}^{4+} + \text{Sn}^{4+}$ ), which could affect oxygen vacancies and unsaturated chemical bonds over the catalyst surface, thus leading to a change of the surface chemisorbed oxygen.

Figure 2 shows the O 1s XPS spectra. All samples exhibit two peaks around 532.0 and 530.0 eV. The peak at binding energies (531–533 eV) corresponded to the surface adsorbed oxygen species (labeled  $\text{O}_a$ ) relating to Ti-OH or Ti-O-V bond, and the band at binding energies (529–531 eV) was attributed to the lattice oxygen species (labeled  $\text{O}_c$ ) relating to Ti-O-Ti bond [26,27]. In the case of V1Mo1 catalysts, the new peak at ca. 531.1 eV mainly corresponded to the surface adsorbed species (labeled  $\text{O}_b$ ) relating to Ti-O-Mo or V-O-Mo bond, demonstrating that the introduction of Mo changed the state of oxygen species and interacted with Ti or V species. The percentage of lattice oxygen species ( $\text{O}_c$ ) of  $\text{V}_2\text{O}_5/\text{TiO}_2$  catalyst was the same to

V1Mo1 sample. After catalytic tests, the percentage of lattice oxygen species of  $V_2O_5/TiO_2$  catalyst increased, while the V1Mo1 sample decreased, implying that Mo reacted with Ti-O-Ti bond to form Ti-O-Mo bond during the catalytic process.

### 3.2. Catalytic activity

The selective oxidation of 2-methylnaphthalene to 2-naphthaldehyde was conducted as a model reaction to evaluate the activities of as-prepared catalysts. The catalytic test results indicated that the main products of the gas oxidation reaction were 2-naphthaldehyde, phthalic anhydride, 4-methylphthalic anhydride, 2-methyl-1,4-naphthoquinone, and 6-methyl-1,4-naphthoquinone. Only a small total oxidation to  $CO_x$  was observed under some conditions and cumulative selectivity to other detected compounds did not exceed 5%. The catalytic activity of all tested samples was stable during tests.

As shown in Fig. 3(a), with the increase of Mo introduction amount, conversion of 2-methylnaphthalene was first increased, then decreased. The optimal value was achieved for the V1Mo1 sample (V/Mo molar ratio, 1:1). The similar phenomenon can be seen in Fig. S6 (ESI) and Fig. 3(b) for selectivity and yield to 2-naphthaldehyde. Importantly, the influence of Mo introduction on selectivity to 2-naphthaldehyde was more obvious than that on conversion of 2-methylnaphthalene for  $V_2O_5/TiO_2$  catalyst. Selectivity to 2-naphthaldehyde decreased with the increase in conversion of 2-methylnaphthalene, quite noticeable for the V1Mo2 sample. Another phenomenon is that selectivity and yield to 2-naphthaldehyde decreased seriously for most catalysts once the reaction temperature reached 400°C. Furthermore, the

catalytic performance of  $V_2Mo_3$  sample (V/Mo molar ratio, 2:3) was very close to  $V_1Mo_1$  sample because of the approximate V/Mo molar ratio.

### 3.3. Possible mechanism of Mo promotional effect

The addition of Mo can significantly alter the activity of  $V_2O_5/TiO_2$  catalyst. Only with the appropriate amount of Mo,  $V_2O_5/TiO_2$  catalyst can acquire the best performance for catalytic oxidation of 2-methylnaphthalene to 2-naphthaldehyde. This result indicates that Mo can enhance or weaken the performance of  $V_2O_5/TiO_2$  catalyst depending on the loading amount. One possible reason is that Mo interacts with V or Sn, even with Ti element. According to the XPS analysis of  $V_2O_5/TiO_2$  and  $V_1Mo_1$  catalysts, the chemical state and composition of V and Sn in the catalyst were changed after the addition of Mo. From the Raman spectra result, Mo interacts with vanadium species and Sn species and decreases the intensity of  $K-O-V=O$  sites and  $SnO_2$ . These subtle variations affect the activity of  $V_2O_5/TiO_2$  catalysts largely. Here we propose a mechanism to explain the enhancing effect of Mo, shown in Fig. 4 and Fig. S7-S8 (ESI). Assuming the polymeric vanadium species as the active agent, vanadium species contain  $V=O$  bonds, bridging  $Ti-O-V$  bonds and one bridging  $K-O-V$  bond. With the addition of Mo, Mo attacks the bridging oxygen and then replaces K to form a new bridging  $Mo-O-V$  bond, or reacts with Ti to form a new  $Mo-O-Ti$  bond. As is shown in Fig S7-S8 (ESI), the terminal  $V=O$  bond and the bridge  $V-O-Ti$  bond participates in the oxidation of 2-methylnaphthalene by transferring of electrons. Moreover, the formation of bridging  $Mo-O-V$  and  $Mo-O-Ti$  bond would decrease the amounts of  $Ti-O-V$  bond, causing the decrease of

vanadium species sites. Under the overdosed Mo introduction, vanadium species sites may decrease badly. This inhibits the activity of  $V_2O_5/TiO_2$  catalyst, leading to a poor performance for V1Mo2 sample. Further investigations will be done to study and verify this reaction mechanism.

#### 4. Conclusion

Introduction of molybdenum to  $V_2O_5/TiO_2$  catalyst has a noticeable effect on the vanadium surface structure. XRD experiment indicates  $KVO_3$  phase gradually disappears with the increase of Mo loadings. The surface states of Ti, V, O, and Sn characterized by XPS are altered by Mo introduction. Catalytic data on the selective oxidation of 2-methylnaphthalene reveals the influence of molybdenum on catalytic performance of  $V_2O_5/TiO_2$  catalyst. The addition of molybdenum (V1Mo1 and V2Mo3) shows an accelerating effect, while other addition shows no promotional effect on the catalytic properties of  $V_2O_5/TiO_2$  catalyst. Molybdenum modified catalysts demonstrate different surface structure and state of vanadium species due to the addition amount. These changes determine the high activity and selectivity in the oxidation of 2-methylnaphthalene into 2-naphthaldehyde for the V1Mo1 sample.

#### References

- [1] M. Ponzi, C. Duschatzky, A. Carrascull, E. Ponzi, *Appl. Catal. A Gen.* 169 (1998)

- 373–379.
- [2] T. Mongkhonsi, L. Kershenbaum, *Appl. Catal. A Gen.* 170 (1998) 33–48.
- [3] J.W. Yoon, S.H. Jhung, J.S. Chang, *Bull. Korean Chem. Soc.* 28 (2007) 2405–2408.
- [4] F. Zhang, X.C. Li, Y.C. Tang, X.Q. Gao, L. Xu, G.J. Liu, *Can. J. Chem. Eng.* 94 (2016) 1184–1190.
- [5] M. Florea, R.S. Marin, F.M. Pălășanu, F. Neațu, V.I. Pârvulescu, *Catal. Today* 254 (2015) 29–35.
- [6] X.Q. Gao, F. Zhang, Y. Yu, Y.H. Dou, L. Xu, G. J. Liu, *J. Chem. Eng. Data* 63 (2018) 2848–2855.
- [7] H.M. Doukas, *J. Chem. Educ.* 31 (1954) 12.
- [8] M. Bollini, J.J. Casal, A.M. Bruno, *Bioorg. Med. Chem.* 16 (2008) 8003–8010.
- [9] E.I. Shimanskaya, E.M. Sulman, V.Y. Doluda, *Catal. Sustain. Energy* 2 (2015) 28–32.
- [10] A. Martin, U. Bentrup, G.U. Wolf, *Appl. Catal. A Gen.* 227 (2002) 131–142.
- [11] A. Martin, *Top. Catal.* 29 (2004) 201–206.
- [12] H.Y. Zhao, S. Bennici, J.Y. Shen, A. Auroux, *Appl. Catal. A Gen.* 356 (2009) 121–128.
- [13] R. Grabowski, B. Grzybowska, K. Samson, J. Słoczyński, J. Stoch, K. Wcisło, *Appl. Catal. A Gen.* 125 (1995) 129–144.
- [14] G.K. Boreskov, A.A. Ivanov, O.M. Ilyinich, V.G. Ponomareva, *React. Kin. Catal. Lett.* 3 (1975) 1–8.

- [15] F. Bertinchamps, C. Grégoire, E.M. Gaigneaux, *Appl. Catal. B Environ.* 66 (2006) 10–22.
- [16] H.K. Matralisa, C. Papadopoulou, Kordulis C, A.A. Elguezabal, V.C. Corberan, *Appl. Catal. A Gen.*126 (1995) 365–380.
- [17] B.M. Reddy, A. Khan, Y. Yamada, T. Kobayashi, S. Loridant, J.C. Volta, *J. Phys. Chem. B.* 107 (2003) 5162–5167.
- [18] L.N. Gan, J.J. Chen, Y. Peng, J. Yu, T. Tran, K.Z. Li, D. Wang, G.W. Xu, J.H. Li, *Ind. Eng. Chem. Res.* 57 (2018) 150–157.
- [19] S.H. Sun, G.W. Meng, G.X. Zhang, T. Gao, B.Y. Geng, L.D. Zhang, J. Zuo, *Chem. Phys. Lett.* 376 (2003) 103–107.
- [20] L. Lietti, I. Nova, G. Ramis, L. Dall'Acqua, G. Busca, E. Giamello, P. Forzatti, F. Bregani, *J. Catal.* 187 (1999) 419–435.
- [21] D.A. Bulushev, F. Rainone, L. Kiwi-Minsker, A. Renken, *Langmuir.* 17 (2001) 5276–5282.
- [22] G.T. Went, S.T. Oyama, A.T. Bell, *J. Phys. Chem.* 94 (1990) 4240–4246.
- [23] P. Eversfeld, W.J. Liu, E. Klemm, *Catal. Lett.* 147 (2017) 785–791.
- [24] J.S. Wang, H. Liu, *RSC. Adv.* 6 (2016) 2374–2378.
- [25] H. Liu, R.Z. Hu, W. Sun, M.Q. Zeng, J.W. Liu, L.C. Yang, M. Zhu, *J. Power. Sources* 242 (2013) 114–121.
- [26] S.H. Zhan, H. Zhang, Y. Zhang, Q. Shi, Y. Li, X.J. Li, *Appl. Catal. B Environ.* 203 (2017) 199–209.
- [27] J.C. Dupin, D. Gonbeau, P. Vinatier, A. Levasseur, *Phys. Chem. Chem. Phys.* 2

(2000) 1319–1324.

ACCEPTED MANUSCRIPT

### **Table Captions**

**Table 1** Textural properties of the different samples (V/Mo ratios =1:0, 6:1, 3:1, 1:1, 2:3, 1:2)

**Table 2** Binding energies and ratios of V, Ti, O, Sn and Mo obtained from XPS spectroscopy

**Table 1** Textural properties of the different samples (V/Mo ratios =1:0, 6:1, 3:1, 1:1, 2:3, 1:2)

Samples	Surface Area(m <sup>2</sup> ·g <sup>-1</sup> )	Average size(nm)	Pore Volume(cm <sup>3</sup> ·g <sup>-1</sup> )
V <sub>2</sub> O <sub>5</sub> /TiO <sub>2</sub>	5.41	37.22	0.050
V6 Mo1	5.56	24.51	0.034
V3 Mo1	3.16	35.42	0.027
V1 Mo1	4.33	28.36	0.011
V2 Mo3	3.42	17.40	0.014
V1 Mo2	1.88	19.68	0.009
V <sub>2</sub> O <sub>5</sub> /TiO <sub>2</sub> used	3.04	13.92	0.011
V1 Mo1 used	4.23	7.55	0.008
V2 Mo3 used	3.24	8.05	0.006

**Table 2** Binding energies and ratios of V, Ti, O, Sn and Mo obtained from XPS spectroscopy

	V <sub>2</sub> O <sub>5</sub> /TiO <sub>2</sub>	V <sub>2</sub> O <sub>5</sub> /TiO <sub>2</sub> used	V1Mo1	V1Mo1 used	Relative species
V 2p <sub>3/2</sub>	517.7 (80)	517.5 (68)	517.7 (92)	517.5 (54)	V <sup>5+</sup>
	516.6 (20)	516.4 (32)	516.6 (8)	516.4 (46)	V <sup>4+</sup>
Ti 2p <sub>3/2</sub>	459.1	458.9	459.0	458.9	Ti <sup>4+</sup>
O 1s	-	-	532.2 (52)	532.1 (48)	Ti-OH, Ti-O-V
	532.3 (76)	532.2 (68)	531.1 (24)	531.0 (37)	Ti-O-Mo, Mo-O-V
	530.3 (24)	530.2 (32)	530.3 (24)	530.2 (15)	Ti-O-Ti
	-	-	-	-	Sn <sup>4+</sup>
3d <sub>5/2</sub>	487.8 (50)	487.6 (31)	486.8	486.5	Sn <sup>2+</sup>
Mo 3d <sub>5/2</sub>	-	-	233.0	232.7	Mo <sup>6+</sup>

### Figure captions

**Fig. 1.** XRD patterns of the V<sub>x</sub>Mo<sub>y</sub> samples: (◆) anatase phase TiO<sub>2</sub>; (○) KVO<sub>3</sub>; (●) rutile phase TiO<sub>2</sub>.

**Fig. 2.** XPS spectra of O 1s over various catalysts.

**Fig. 3.** Conversion of 2-methylnaphthalene (a) and selectivity to 2-naphthaldehyde (b) over  $V_xMoy-TiO_2$  catalysts.

**Fig. 4.** Proposed mechanism of Mo introduction over  $V_xMoy-TiO_2$  catalysts.

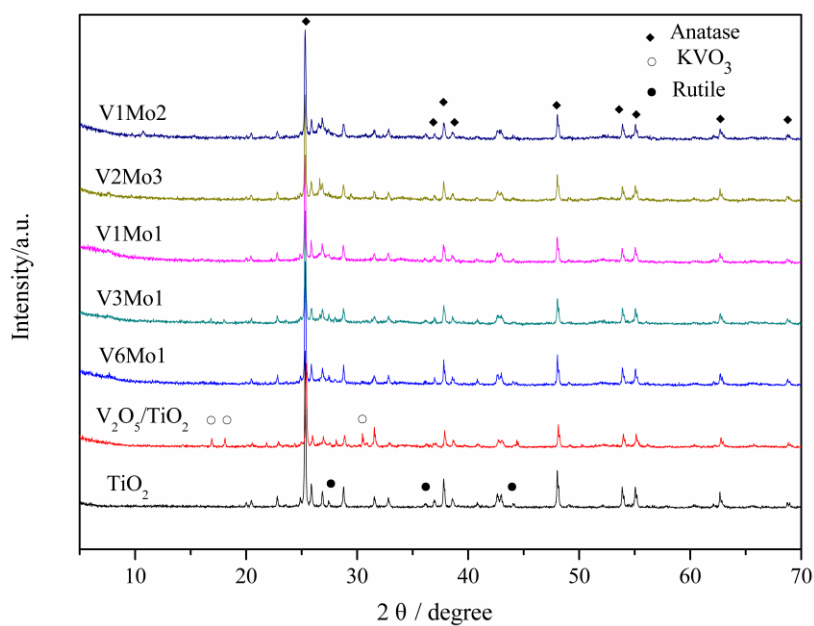


**Fig. 1.** XRD patterns of the  $V_xMoy$  samples: (◆) anatase phase  $TiO_2$ ; (○)  $KVO_3$ ; (●) rutile phase  $TiO_2$ .

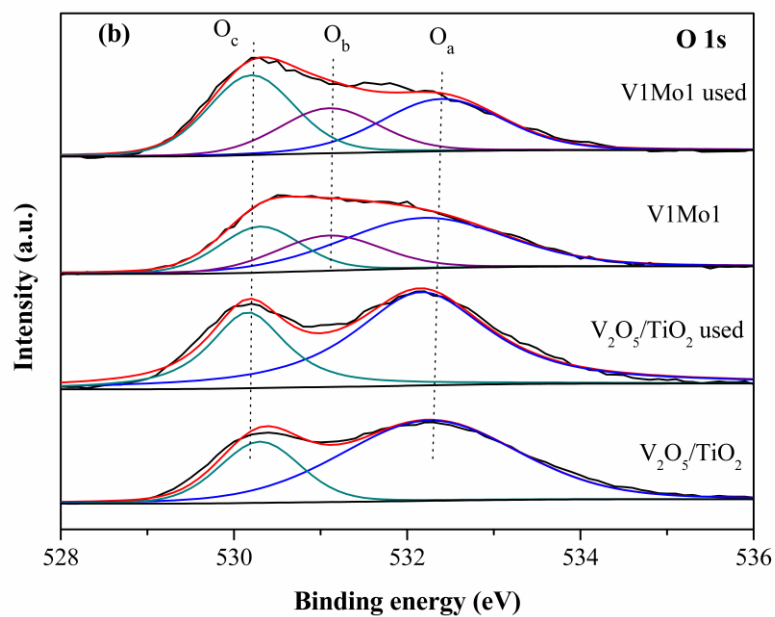
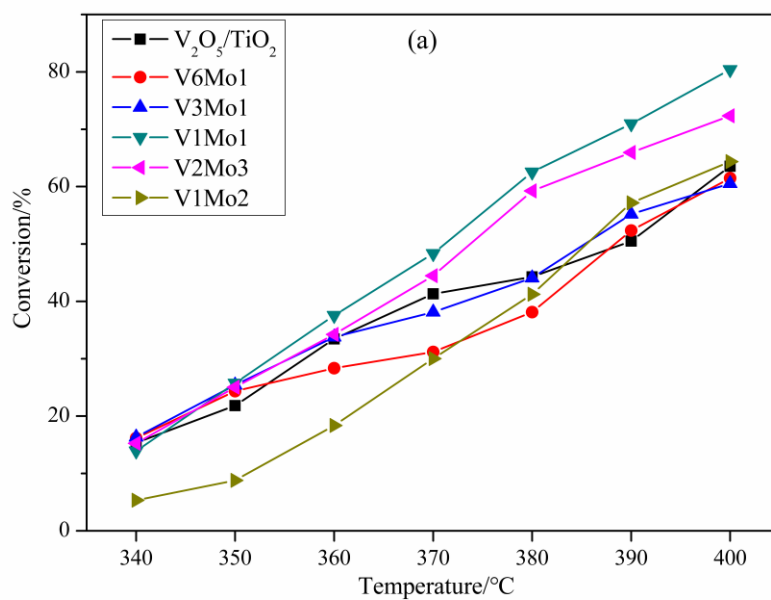
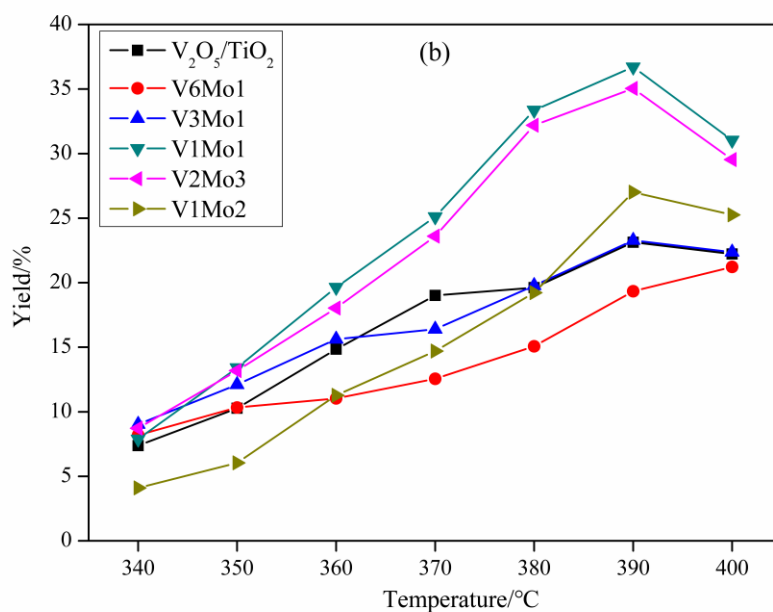
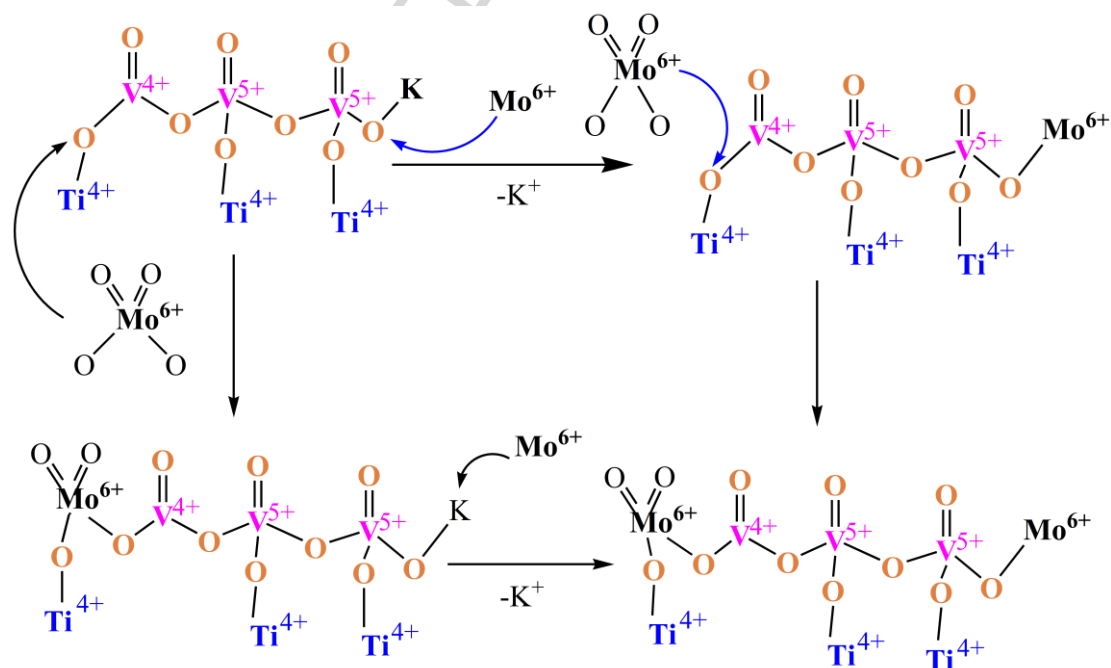


Fig. 2. XPS spectra of O 1s over various catalysts.





**Fig. 3.** Conversion of 2-methylnaphthalene (a) and yield to 2-naphthaldehyde (b) over V<sub>x</sub>Mo<sub>y</sub>-TiO<sub>2</sub> catalysts.



**Fig. 4.** Proposed mechanism of Mo introduction over V<sub>x</sub>Mo<sub>y</sub>-TiO<sub>2</sub> catalysts.

**Highlights**

- Mo-modified  $V_2O_5/TiO_2$  catalysts were prepared by wetness impregnation method.
- Catalysts were tested via oxidizing 2-MN to 2-naphthaldehyde by fixed bed reactor.
- Mo introduction affects the conversion and selectivity of  $V_2O_5/TiO_2$  catalysts.